



Mid-Cenozoic Pacific plate motion change: Implications for the Northwest Hawaiian Ridge and circum-Pacific

Brian R. Jicha^{1*}, Michael O. Garcia², and Paul Wessel²¹Department of Geoscience, University of Wisconsin–Madison, Madison, Wisconsin 53706, USA²Department of Earth Sciences, School of Ocean and Earth Science and Technology (SOEST), University of Hawai‘i at Mānoa, Honolulu, Hawaii 96822, USA

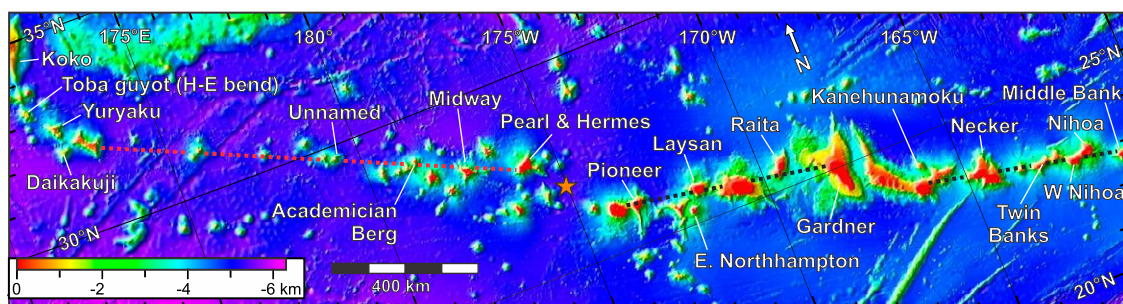
ABSTRACT

The alignment and age progression of volcanoes produced as a tectonic plate moves over a mantle plume can be used to reconstruct both the direction and rate of past plate motion assuming the plume remains in a fixed location. New $^{40}\text{Ar}/^{39}\text{Ar}$ dates for lavas from 15 volcanoes spanning the entire length (~2800 km) of the Northwest Hawaiian Ridge (NWHR) facilitate improved age-distance relationships. These are used to constrain a significant kink in the NWHR at 25.3 ± 0.5 Ma as the Pacific plate experienced a brief episode of more northerly motion and rotated counter-clockwise. The age progression (i.e., velocity of the Pacific plate) increased markedly from 57 to 87 km/Ma following the plate motion change. This mid-Cenozoic tectonic reorganization has been previously identified in plate motion models, but has been poorly constrained temporally. We demonstrate that this event affected four seamount trails within the Pacific Basin, and had a significant impact on all circum-Pacific volcanic arcs.

INTRODUCTION

The Hawaiian-Emperor chain is one of the longest intraplate seamount trails, extending for more than 6000 km and >80 Ma. It can be subdivided into three main segments: the Emperor Seamounts (north of the Hawaiian-Emperor bend [HEB]; 82–50 Ma), the Northwest Hawaiian Ridge (NWHR, south of the bend to Middle Bank Seamount; 49–6 Ma), and the Hawaiian Islands (Ni‘ihau to the Island of Hawai‘i; <6 Ma). The Emperor seamount track has been attributed, in part, to southward motion of the mantle plume (Tarduno et al., 2003). Relatively minor hotspot drift is assumed after the HEB, implying plate motion should produce a linear track of NWHR volcanoes. However, several kinks exist along the NWHR, the most prominent of which is the focus of this study.

Figure 1. Map of Northwest Hawaiian Ridge (north Pacific Ocean) showing dated volcanoes and those mentioned in the text. Orange star denotes approximate location of mid-Cenozoic plate motion change. Seamounts to the south of the Pearl and Hermes atoll are Cretaceous in age (O’Connor et al., 2013).



Relief grid is the 30 arc sec global compilation of Becker et al. (2009).

*E-mail: brian.jicha@wisc.edu

CITATION: Jicha, B.R., Garcia, M.O., and Wessel, P., 2018, Mid-Cenozoic Pacific plate motion change: Implications for the Northwest Hawaiian Ridge and circum-Pacific: *Geology*, v. 46, p. 939–942, <https://doi.org/10.1130/G45175.1>

TABLE 1. SUMMARY OF $^{40}\text{Ar}/^{39}\text{Ar}$ DATA

Sample #	Volcano	km from Kīlauea volcano	Stage	No. of expts*	Total fusion age (Ma $\pm 2\sigma$)	$^{40}\text{Ar}/^{39}\text{Ar}$ ($\pm 2\sigma$)	Isochron age (Ma $\pm 2\sigma$)	N	^{39}Ar (%)	MSWD	Plateau age (Ma $\pm 2\sigma$)
A-53-1	Yuryaku	3541	S	2	47.91 \pm 0.22	300.4 \pm 4.3	47.63 \pm 0.31	19 of 21	97.8	0.83	47.88 \pm 0.21
A-53-2	Yuryaku	3541	—	2	31.21 \pm 0.11	295.6 \pm 1.9	31.00 \pm 0.10	15 of 24	71.9	0.80	31.01 \pm 0.10
A-55-4	Daikakuji	3520	S	1	46.86 \pm 0.31	322.0 \pm 40.0	46.68 \pm 0.67	11 of 15	90.4	0.79	47.60 \pm 0.30
A-55-2	Daikakuji	3520	S	1	45.84 \pm 0.20	300.6 \pm 6.7	46.67 \pm 0.49	6 of 10	54.2	0.67	46.99 \pm 0.25
A-55-1	Daikakuji	3520	S	2	46.97 \pm 0.20	303.1 \pm 8.5	46.38 \pm 0.54	19 of 23	89.6	0.49	46.83 \pm 0.20
84-28-B	Unnamed	2801	PS	1	32.99 \pm 0.16	292.8 \pm 11.6	32.82 \pm 0.34	7 of 10	63.5	1.09	32.76 \pm 0.16
84-30-J	Academician Berg	2608	S	2	33.31 \pm 0.43	296.4 \pm 4.1	32.65 \pm 0.85	20 of 22	91.5	0.65	32.82 \pm 0.40
72-20-AA	Academician Berg	2608	PS	2	30.70 \pm 0.29	299.4 \pm 1.5	30.91 \pm 0.15	13 of 27	71.2	0.75	31.40 \pm 0.14
72-20-C1	Academician Berg	2608	PS	1	31.06 \pm 0.26	302.3 \pm 22.7	31.87 \pm 0.22	8 of 8	100.0	0.80	31.09 \pm 0.22
72-20-A1	Academician Berg	2608	PS	1	32.11 \pm 0.21	302.3 \pm 22.7	31.87 \pm 0.22	6 of 10	85.0	1.08	31.91 \pm 0.17
76-5-4-A	E Northhampton	1846	S	1	23.11 \pm 0.22	297.7 \pm 4.9	23.20 \pm 2.30	27 of 27	100.0	1.04	23.11 \pm 0.23
P5-530-3	Laysan	1831	S	1	20.92 \pm 0.14	297.5 \pm 3.2	21.07 \pm 0.11	8 of 10	87.6	0.91	21.09 \pm 0.11
P5-530-1	Laysan	1831	PS	1	20.63 \pm 0.05	290.7 \pm 9.4	20.61 \pm 0.05	7 of 10	91.5	0.32	20.60 \pm 0.05
P5-538-1	Raita	1611	PS	2	17.62 \pm 0.05	293.7 \pm 6.0	18.06 \pm 0.05	15 of 22	80.7	0.53	18.05 \pm 0.05
76-6-7-H	Gardner	1449	S	1	14.45 \pm 0.14	297.9 \pm 2.0	14.10 \pm 0.58	10 of 13	77.5	0.98	14.11 \pm 0.16
72-37-C	Gardner	1449	RJ	2	12.55 \pm 0.19	296.5 \pm 2.8	12.42 \pm 0.18	22 of 23	92.9	0.99	12.46 \pm 0.13
72-41-B	Brooks	1302	RJ	2	13.05 \pm 0.05	299.5 \pm 1.7	12.69 \pm 0.16	19 of 23	79.0	1.07	12.86 \pm 0.06
P5-701-4	Kānehuamoku	1235	PS	1	12.97 \pm 0.03	318.6 \pm 59.4	13.48 \pm 0.13	5 of 11	72.8	0.70	13.53 \pm 0.03
P5-701-2	Kānehuamoku	1235	PS	1	13.01 \pm 0.05	294.0 \pm 14.9	13.34 \pm 0.29	7 of 12	77.0	1.07	13.31 \pm 0.05
NEC-3A	Mokumanamana	1080	S	2	12.15 \pm 0.13	296.4 \pm 2.3	12.10 \pm 0.12	19 of 19	100.0	0.62	12.13 \pm 0.09
P5-544-4	Mokumanamana	1080	PS	1	9.90 \pm 0.01	265.7 \pm 107.7	9.94 \pm 0.03	11 of 15	88.3	0.70	9.93 \pm 0.01
72-51-D	Twin Banks	920	PS	2	9.40 \pm 0.10	294.5 \pm 11.0	9.04 \pm 0.24	18 of 22	70.3	0.83	9.01 \pm 0.07
76-9-11	West Nihoa	825	PS	1	7.90 \pm 0.03	301.9 \pm 3.9	8.02 \pm 0.07	7 of 14	57.8	0.48	8.19 \pm 0.03
NIH-D-1-2	Nihoa	794	S	2	8.34 \pm 0.09	296.9 \pm 3.5	8.40 \pm 0.09	18 of 22	96.8	0.99	8.42 \pm 0.07
J230319	Middle Bank	702	PS	1	5.89 \pm 0.08	298.2 \pm 4.8	5.90 \pm 0.15	9 of 10	84.5	1.29	5.95 \pm 0.08
J230126	Middle Bank	702	PS	1	5.52 \pm 0.10	294.2 \pm 2.6	5.64 \pm 0.15	9 of 10	94.3	0.23	5.58 \pm 0.09

Note: Ages calculated relative to 28.201 Ma Fish Canyon sanidine standard using decay constants of Min et al. (2000). Plateau ages are preferred. See text for discussion. Stage: S—shield, PS—post-shield, RJ—rejuvenation. Note that sample A-53-2 is an intraplate basalt.

(2013) to speculate that there are two distinct age trends along the NWHR, with an apparent doubling of the rate of plate motion since 15 Ma and possibly as early as ca. 27 Ma. This assertion was made without any new $^{40}\text{Ar}/^{39}\text{Ar}$ data from lavas younger than 25 Ma.

$^{40}\text{Ar}/^{39}\text{Ar}$ METHODS AND RESULTS

We obtained 26 new $^{40}\text{Ar}/^{39}\text{Ar}$ dates from 15 volcanoes from Yuryaku seamount (near the HEB) to Middle Bank seamount (Fig. 1). When possible, fresh plagioclase was isolated from the NWHR samples. In lieu of abundant plagioclase, holocrystalline groundmass was utilized. We conducted initial incremental heating experiments using a resistance furnace or a 25W CO_2 laser, and analyzed the gas using a MAP215–50 mass spectrometer (e.g., Jicha and Brown, 2014). Four samples were analyzed using both the furnace and the laser, and the results are nearly identical in all cases. Subsequent experiments were conducted using a 60W CO_2 laser and the Noblesse multicollector mass spectrometer (e.g., Jicha et al., 2016). Three samples were analyzed using both mass spectrometers, and the results are indistinguishable. All ages are calculated (including previously published ages mentioned herein) using a Fish Canyon Tuff sanidine standard age of 28.201 \pm 0.046 Ma (Kuiper et al., 2008) and the decay constants of Min et al. (2000) (Table 1). Because all of the isochrons have intercepts that are within uncertainty of the atmospheric value, the plateau ages are preferred. Complete argon isotope data, full analytical and sample preparation details, and whole-rock X-ray fluorescence (XRF) data are available in the GSA Data Repository¹.

AGE OF THE HAWAIIAN-EMPEROR BEND

Linear age-versus-distance relationships were calculated using the new $^{40}\text{Ar}/^{39}\text{Ar}$ data to assess changes in Pacific plate motion for several segments of the NWHR. Age regressions are for shield-stage lavas only, as they most likely reflect the time when the vertical stem of the hotspot was located beneath or close to the seamount. From Koko (north) seamount (52.9 Ma) to Midway island (27.8 Ma), the age progression is 57 km/Ma

(Fig. 2), which is identical to the rate calculated by O'Connor et al. (2013) for this segment. This rate is used to determine an updated estimate of the HEB. Both Sharp and Clague (2006) and O'Connor et al. (2013) suggest that the HEB is an arcuate feature that formed over several million years beginning at 50 Ma and ending by 47.5 Ma (O'Connor et al., 2013) or 42 Ma (Sharp and Clague, 2006). We suggest HEB formation may have been more rapid, with a location at the apex in the Emperor chain and NWHR at Toba Guyot (Fig. 1). Toba is located ~85 km northwest of Yuryaku seamount. Our oldest $^{40}\text{Ar}/^{39}\text{Ar}$ age from Yuryaku is 47.88 \pm 0.21 Ma (Figs. 1 and 2). Extrapolating the 57 km/Ma rate from Yuryaku to Toba Guyot gives an age of 49.4 \pm 0.4 Ma for the HEB. Our 49.4 Ma HEB age is ~2 Ma younger than the 51–52 Ma U-Pb zircon ages from forearc gabbros in the Izu-Bonin-Mariana (Ishizuka et al., 2011) and Tonga arc systems (Meffre et al., 2012) that are associated with subduction initiation along the western edge of the Pacific plate. Because the HEB is likely the result of changes in both plate and hotspot motions (e.g., O'Connor et al., 2013), and because it is not yet possible to deconvolve these two processes, it remains difficult to properly assess the temporal relationship between the HEB and western Pacific subduction initiation.

MID-CENOZOIC PACIFIC PLATE MOTION CHANGE

Pacific plate motion changes following the HEB have been documented for decades (e.g., Atwater, 1970). An ~8–15° counter-clockwise rotation of the Pacific plate in the mid-Cenozoic likely resulted in the ~150 km southward offset or kink in the NWHR east of Pearl and Hermes atoll (e.g., Lonsdale, 1986; Croon et al., 2008) (Fig. 1). Our <21 Ma and 52–28 Ma age progression rates are extrapolated to the inferred location of this plate motion change (~2235 km from Kīlauea volcano, Hawaii; orange star in Fig. 2), and establish an age of 25.3 \pm 0.5 Ma (Fig. 2). The age progression from Laysan island (21.1 Ma) through the Hawaiian Islands increased markedly to 87 km/Ma compared to 57 km/Ma before the plate motion change (Fig. 2). Thus, at 25.3 Ma, there was a directional change in plate motion and a spreading rate or plate velocity increase.

¹GSA Data Repository item 2018344, File DR1: $^{40}\text{Ar}/^{39}\text{Ar}$ plateau and inverse isochron diagrams for all dated NWHR samples; File DR2: Total alkali vs. SiO_2 diagram for all dated NWHR samples. The blue dividing line for separating alkali (above) from tholeiitic (below) lavas is from Macdonald and Katsura (1964); File DR3: XRF analyses of dated NWHR lavas, is available online at <http://www.geosociety.org/datarerepository/2018/> or on request from editing@geosociety.org.

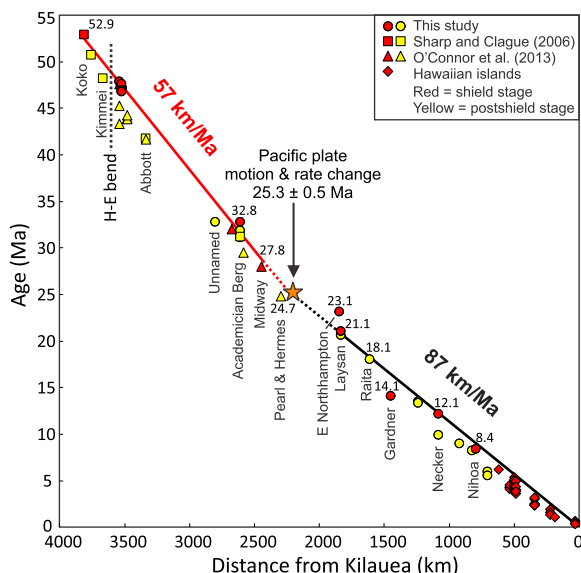


Figure 2. Distance from Kilauea volcano, Hawaii, versus age using recent $^{40}\text{Ar}/^{39}\text{Ar}$ ages for Northwest Hawaiian Ridge (NWHR), southern Emperor seamount chain, and Hawaiian Island volcanoes. The 53–28 Ma age progression (57 km/Ma) includes southern Emperor volcanoes continuing southeast through Midway. The younger trend (Laysan to Kilauea, 21–0 Ma) gives a faster rate (87 km/Ma). Linear age regressions are for shield-stage lavas only. For volcanoes with multiple shield-stage ages, only the oldest one was used for the regressions. Hawaiian island age and geochemical data are from Ito et al. (2013) and Garcia et al. (2015, and references therein).

CIRCUM-PACIFIC IMPLICATIONS

Dott (1969) was among the first to suggest that many circum-Pacific continental and island arcs contain evidence of a mid-Cenozoic (30–25 Ma) “structural disturbance” that should also be reflected in the Pacific seafloor. Numerous subsequent studies throughout the Pacific Basin have also called upon a mid-Cenozoic change in direction of the Pacific Plate (e.g., Handschumacher, 1976; Wessel et al., 2006). This major change in plate direction and velocity is typically mentioned in passing because the timing of this event, until now, was loosely constrained to 28–24 Ma. However, with more precise and accurate geochronologic data generated for a variety of applications in the Pacific Basin, it is now possible to re-evaluate the potential link between mid-Cenozoic events throughout the circum-Pacific and the reorientation of the Pacific Plate at 25.3 Ma.

Based on tectonic reconstructions and magnetic anomaly patterns, Handschumacher (1976) suggested that the Farallon Plate was broken up into the Nazca, Gorda, and Cocos Plates in the eastern Pacific Basin at ca. 25 Ma. Spreading along the Nazca Ridge ceased at ca. 25 Ma and volcanism along the Easter Seamount chain began following a change in the direction of motion of the Nazca plate. Post-shield lavas near the elbow or bend in the Nazca Ridge–Easter seamount chain have $^{40}\text{Ar}/^{39}\text{Ar}$ ages as old as 25.1 ± 0.2 Ma (Ray et al., 2012), which are consistent with our 25.3 Ma age for Pacific plate motion change. Other ca. 25 Ma events in the eastern Pacific that have been attributed to Farallon slab breakup or a basin-wide tectonic reorganization include (1) the second pulse of the silicic large igneous province in the Sierra Madre Occidental, Mexico (Ferrari et al., 2007), and (2) the switch from slower (7 cm/yr), oblique South America–Farallon convergence to more rapid (15 cm/yr), nearly orthogonal Nazca–South American convergence during the initial uplift of the modern Andes. Some of the first eruptions in central Chile associated with this subduction change are dated at 23.9 ± 0.1 Ma (Kay and Copeland, 2006).

Along the northern edge of the Pacific plate at the Pacific–North America plate boundary, rapid exhumation along the Denali fault system and the

eastern Alaska Range was initiated at ca. 25 Ma (Benowitz et al., 2013). The driving mechanism for this deformation is attributed to the Pacific plate and Yakutat microplate, both of which likely transferred strain inland to Alaska (Benowitz et al., 2013). Within the Cobb seamount chain in the Gulf of Alaska, the 23.1 Ma Pathfinder seamount is located ~500 km to the southeast of the 27.6 Ma Murray seamount, with an apparent gap in volcanism between the two seamounts (Duncan and Clague, 1985; Dalrymple et al., 1987). The direction of the offset to the southeast, as well as the timing of it, are similar to what is observed in the NWHR. Counter-clockwise rotation of the Pacific plate at 25.3 Ma would have resulted in subduction that is more oblique than present-day subduction in the central Aleutian arc, thereby delivering less subducted material to the mantle and likely slowing magma production. This may explain the apparent lack of volcanic and plutonic rocks emplaced from 26 to 18 Ma in the central Aleutian Islands (Jicha and Kay, 2018).

At ca. 25 Ma in the western Pacific, volcanism ceased along the entire ~2800 km length of the Kyushu–Palau arc as rifting began to form the Shikoku and Parece Vela basins, thereby isolating the Kyushu–Palau Ridge from the volcanic front (Ishizuka et al., 2011). Kasuga and Ohara (1997) proposed that more oblique subduction due to a spreading direction change in the Pacific plate caused strike-slip movement that began to sever the arc, which is consistent with our proposed timing of a shift in plate motion.

In the southwest Pacific, the younger of the two bends in the Louisville hotspot trail, referred to as the 161° W bend, formed between seamounts $^{40}\text{Ar}/^{39}\text{Ar}$ dated at 26.0 and 24.6 Ma (Koppers et al., 2011), which is nearly identical to our temporal constraints for the kink in the NWHR. We note that the shifts or offsets in Louisville, NWHR, and Cobb at ca. 25 Ma are larger toward the north, as captured by the plate motion model WK08-G of Wessel and Kroenke (2008).

To the west of the Louisville hotspot trail lies the transform boundary between the Pacific and Indo-Australia plates. It is widely regarded that propagation of the Alpine fault through the South Island of New Zealand began in the mid-Cenozoic (e.g., Sutherland, 1995). A lamprophyre dike swarm, with U–Pb dates as old as 24.6 Ma, is interpreted to have been emplaced during the initial stages of dextral shear along the Alpine fault (Cooper et al., 1987). Formation of the modern Pacific–Australia plate boundary in New Zealand has been inferred to be coincident with a marked change in the Pacific–Antarctic plate motion (Sutherland, 1995; Cande and Stock, 2004; Croon et al., 2008) and abrupt shortening near the southern terminus of the East Pacific rise (Lonsdale, 1986). All of these events may be associated with the ca. 25 Ma tectonic reorganization in the Pacific Basin.

CAUSE OF PACIFIC PLATE REORIENTATION AND CONCLUSIONS

What triggered the major plate reorganization at 25.3 Ma? Most regional studies of mid-Cenozoic volcanologic or tectonic features in the Pacific basin assumed they were local features and not part of a Pacific-wide phenomenon. Atwater (1970) and Mammerickx and Klitgord (1982) suggested that the mid-Cenozoic plate reorientation was triggered by the intersection of the Pacific–Farallon spreading center with western North America just south of the Mendocino fracture zone. However, it is difficult to envision how an event along the eastern edge of the Pacific plate is responsible for the changes in strike observed in several hotspot trails in the central and southern Pacific Basin. Alternatively, collision of the young, buoyant South Caroline Ridge with the Manus trench ended subduction along the Melanesian arc, forced ‘soft docking’ of the Ontong Java Plateau against the North Solomon block, and may have caused the Pacific plate to be forced northward by the Australia plate (Petterson et al., 1997; Gına and Müller, 2007). This northward shift in the Pacific plate is consistent with the southward offsets in both the NWHR and Cobb seamount chain and the minor offset in the Louisville chain (e.g., Petterson et al., 1997).

In summary, 26 new $^{40}\text{Ar}/^{39}\text{Ar}$ dates from the NWHR indicate that a major tectonic event occurred in the Pacific Basin at 25.3 ± 0.5 Ma,

resulting in a northward jump and counter-clockwise rotation of the Pacific plate. Spreading rate and/or plate velocity increased markedly from 57 km/Ma to 87 km/Ma following this reorientation. Age progression rate calculations suggest the HEB age is 49.4 ± 0.4 Ma. We contend that the ca. 25 Ma plate reorientation was likely more significant than the one associated with the HEB because it can be linked to many volcanic and tectonic events throughout the circum-Pacific, and it affected four (NWHR, Cobb, Easter-Nazca, Louisville) hotspot tracks within the Pacific Basin.

ACKNOWLEDGMENTS

This research was supported by National Science Foundation grants EAR-1219955, OCE-1834758, and OCE-1834723. Jonathon Tree, Zac Olds, and Lauren Froberg aided with sample preparation, and Alexandra Hangsterfer located samples from Scripps Institution of Oceanography collection. We thank John O'Connor, Dave Scholl, and an anonymous reviewer for helpful reviews.

REFERENCES CITED

Atwater, T., 1970, Implications of plate tectonics for the Cenozoic tectonic evolution of western North America: *Geological Society of America Bulletin*, v. 81, p. 3513–3536, [https://doi.org/10.1130/0016-7606\(1970\)81\[3513:IOPTFT\]2.0.CO;2](https://doi.org/10.1130/0016-7606(1970)81[3513:IOPTFT]2.0.CO;2).

Becker, J.J., et al., 2009, Global bathymetry and elevation data at 30 Arc seconds resolution: SRTM30_Plus: *Marine Geodesy*, v. 32, p. 355–371, <https://doi.org/10.1080/01490410903297766>.

Benowitz, J.A., Layer, P.W., and Vanlaningham, S., 2013, Persistent long-term (~24 Ma) exhumation in the Eastern Alaska Range constrained by stacked thermochronology, in Jourdan, F., et al., *Advances in $^{40}\text{Ar}/^{39}\text{Ar}$ Dating: From Archaeology to Planetary Sciences*: Geological Society of London Special Publications, v. 378, p. 225–243, <https://doi.org/10.1144/SP378.12>.

Cande, S.C., and Stock, J.M., 2004, Pacific–Antarctic–Australia motion and the formation of the Macquarie Plate: *Geophysical Journal International*, v. 157, p. 399–414, <https://doi.org/10.1111/j.1365-246X.2004.02224.x>.

Cooper, A.F., Barreiro, B.A., Kimbrough, D.L., and Mattinson, J.M., 1987, Lamprophyre dike intrusion and the age of the Alpine Fault, New Zealand: *Geology*, v. 15, p. 941–944, [https://doi.org/10.1130/0091-7613\(1987\)15<941:LDIATA>2.0.CO;2](https://doi.org/10.1130/0091-7613(1987)15<941:LDIATA>2.0.CO;2).

Croon, M.B., Cande, S.C., and Stock, J.M., 2008, Revised Pacific–Antarctic plate motions and geophysics of the Menard Fracture Zone: *Geochemistry Geophysics Geosystems*, v. 9, Q07001, <https://doi.org/10.1029/2008GC002019>.

Dalrymple, G.B., Clague, D.A., Vallier, T.L., and Menard, H.W., 1987, $^{40}\text{Ar}/^{39}\text{Ar}$ age, petrology and tectonic significance of some seamounts in the Gulf of Alaska, in Keating, B., et al., eds., *Seamounts, Islands, and Atolls: American Geophysical Union Geophysical Monographs*, v. 43, p. 297–315.

Dott, R.H., Jr., 1969, Circum-Pacific late Cenozoic structural rejuvenation: Implications for sea floor spreading: *Science*, v. 166, p. 874–876, <https://doi.org/10.1126/science.166.3907.874>.

Duncan, R.A., and Clague, D.A., 1985, Pacific Plate motion recorded by linear volcanic chains, in Nairn, A.E.M., et al., eds., *The Ocean Basins and Margins*: Boston, Massachusetts, Springer, p. 89–121, https://doi.org/10.1007/978-1-4613-2351-8_3.

Epp, D., 1984, Possible perturbations to hotspot traces and implications for the origin and structure of the Line Islands: *Journal of Geophysical Research*, v. 89, p. 11273–11286, <https://doi.org/10.1029/JB089iB13p11273>.

Ferrari, L., Valencia-Moreno, M., and Bryan, S., 2007, Magmatism and tectonics of the Sierra Madre Occidental and its relation with the evolution of western margin of North America, in Alaniz-Álvarez, S.A., and Nieto-Samaniego, Á.F., eds., *Geology of Mexico: Celebrating the Centenary of the Geological Society of Mexico*: Geological Society of America Special Papers, v. 442, p. 1–39.

Gaina, C., and Müller, D., 2007, Cenozoic tectonic and depth/age evolution of the Indonesian gateway and associated back arc basins: *Earth-Science Reviews*, v. 83, p. 177–203, <https://doi.org/10.1016/j.earscirev.2007.04.004>.

Garcia, M.O., Smith, J.R., Tree, J.P., Weis, D., Harrison, L., and Jicha, B.R., 2015, Petrology, geochemistry, and ages of lavas from Northwest Hawaiian Ridge volcanoes, in Neal, C.R., et al., eds., *The Origin, Evolution, and Environmental Impact of Oceanic Large Igneous Provinces*: Geological Society of America Special Papers, v. 511, p. 1–25, [https://doi.org/10.1130/2015.2511\(01\)](https://doi.org/10.1130/2015.2511(01)).

Handschumacher, D.W., 1976, Post-Eocene plate tectonics of the eastern Pacific, in Sutton, G. H., et al., eds., *The Geophysics of the Pacific Ocean Basin and Its Margin*: American Geophysical Union, Geophysical Monographs, v. 19, p. 177–202, <https://doi.org/10.1029/GM019p0177>.

Ishizuka, O., Taylor, R.N., Yuasa, M., and Ohara, Y., 2011, Making and breaking an island arc: A new perspective from the Oligocene Kyushu–Palau arc, Philippine Sea: *Geochemistry Geophysics Geosystems*, v. 12, Q05005, <https://doi.org/10.1029/2010GC003440>.

Ito, G., Garcia, M., Smith, J., Taylor, B., Flinders, A., Jicha, B., Yamasaki, S., Weis, D., Swinnard, L., and Blay, C., 2013, A low relief shield volcano origin for the South Kaua'i Swell: *Geochemistry Geophysics Geosystems*, v. 14, p. 2328–2348, <https://doi.org/10.1002/ggge.20159>.

Jicha, B.R., and Brown, F.H., 2014, An age on the Korath Range and the viability of $^{40}\text{Ar}/^{39}\text{Ar}$ dating of kaersutite in Late Pleistocene volcanics, Ethiopia: *Quaternary Geochronology*, v. 21, p. 53–57, <https://doi.org/10.1016/j.quageo.2013.03.007>.

Jicha, B.R., and Kay, S.M., 2018, Quantifying subduction erosion and the northward migration of volcanism in the central Aleutian arc: *Journal of Volcanology and Geothermal Research*, v. 360, p. 84–99, <https://doi.org/10.1016/j.jvolgeores.2018.06.016>.

Jicha, B.R., Singer, B.S., and Sobol, P., 2016, Re-evaluation of the ages of $^{40}\text{Ar}/^{39}\text{Ar}$ sanidine standards and supereruptions in the western U.S. using a Noblesse multi-collector mass spectrometer: *Chemical Geology*, v. 431, p. 54–66, <https://doi.org/10.1016/j.chemgeo.2016.03.024>.

Kamp, P.J.J., 1991, Late Oligocene Pacific-wide tectonic event: *Terra Nova*, v. 3, p. 65–69, <https://doi.org/10.1111/j.1365-3121.1991.tb00845.x>.

Kasuga, S., and Ohara, Y., 1997, A new model of back-arc spreading in the Parece Vela Basin, northwest Pacific margin: *The Island Arc*, v. 6, p. 316–326, <https://doi.org/10.1111/j.1440-1738.1997.tb00181.x>.

Kay, S.M., and Copeland, P., 2006, Early to middle Miocene backarc magmas of the Neuquén Basin: Geochemical consequences of slab shallowing and the westward drift of South America, in Kay, S.M., and Ramos, V.A., eds., *Evolution of an Andean Margin: A Tectonic and Magmatic View from the Andes to the Neuquén Basin (35°–39°S Lat.): Geological Society of America Special Papers*, v. 407, p. 185–213, [https://doi.org/10.1130/2006.2407\(09\)](https://doi.org/10.1130/2006.2407(09)).

Koppers, A.A.P., Gowen, M.D., Colwell, L.E., Gee, J.S., Lonsdale, P.F., Mahoney, J. J., and Duncan, R.A., 2011, New $^{40}\text{Ar}/^{39}\text{Ar}$ age progression for the Louisville hot spot trail and implications for inter-hot spot motion: *Geochemistry Geophysics Geosystems*, v. 12, Q0AM02, <https://doi.org/10.1029/2011GC003804>.

Kuiper, K.F., Deino, A., Hilgen, F.J., Krijgsman, W., Renne, P.R., and Wijbrans, J.R., 2008, Synchronizing rock clocks of Earth history: *Science*, v. 320, p. 500–504, <https://doi.org/10.1126/science.1154339>.

Lonsdale, P., 1986, Tectonic and magmatic ridges in the Eltanin fault system, South Pacific: *Marine Geophysical Researches*, v. 8, p. 203–242, <https://doi.org/10.1007/BF00305484>.

Lonsdale, P., 1988, Geography and history of the Louisville hotspot chain in the Southwest Pacific: *Journal of Geophysical Research*, v. 93, p. 3078–3104, <https://doi.org/10.1029/JB093iB04p03078>.

Mammerickx, J., and Klitgord, K.D., 1982, Northern East Pacific Rise: Evolution from 25 m.y. B.P. to the present: *Journal of Geophysical Research*, v. 87, p. 6751–6759, <https://doi.org/10.1029/JB087iB08p06751>.

Meffre, S., Falloon, T.J., Crawford, T.J., Hoernle, K., Hauff, F., Duncan, R.A., Bloomer, S.H., and Wright, D.J., 2012, Basalts erupted along the Tongan fore arc during subduction initiation: Evidence from geochronology of dredged rocks from the Tonga fore arc and trench: *Geochemistry Geophysics Geosystems*, v. 13, Q12003, <https://doi.org/10.1029/2012GC004335>.

Min, K., Mundil, R., Renne, P.R., and Ludwig, K.R., 2000, A test for systematic errors in $^{40}\text{Ar}/^{39}\text{Ar}$ geochronology through comparison with U/Pb analysis of a 1.1-Ga rhyolite: *Geochimica et Cosmochimica Acta*, v. 64, p. 73–98, [https://doi.org/10.1016/S0016-7037\(99\)00204-5](https://doi.org/10.1016/S0016-7037(99)00204-5).

O'Connor, J.M., Steinberger, B., Regelous, M., Koppers, A.A.P., Wijbrans, J.R., Haase, K.M., Stoffers, P., Jokat, W., and Garbe-Schönberg, D., 2013, Constraints on past plate and mantle motion from new ages for the Hawaiian–Emperor Seamount Chain: *Geochemistry Geophysics Geosystems*, v. 14, p. 4564–4584, <https://doi.org/10.1002/ggge.20267>.

Petterson, M.G., Neal, C.R., Mahoney, J.J., Kroenke, L.W., Saunders, A.D., Babbs, T.L., Duncan, R.A., Tolia, D., and McGrail, B., 1997, Structure and deformation of north and central Malaita, Solomon Islands: Tectonic implications for the Ontong Java Plateau–Solomon Arc collision, and for the fate of oceanic plateaus: *Tectonophysics*, v. 283, p. 1–33, [https://doi.org/10.1016/S0040-1951\(97\)00206-0](https://doi.org/10.1016/S0040-1951(97)00206-0).

Ray, J.S., Mahoney, J.J., Duncan, R.A., Ray, J., Wessel, P., and Naar, D.F., 2012, Chronology and geochemistry of lavas from the Nazca Ridge and Easter seamount chain: An ~30 Myr hotspot record: *Journal of Petrology*, v. 53, p. 1417–1448, <https://doi.org/10.1093/petrology/egs021>.

Sharp, W.D., and Clague, D., 2006, 50-Ma initiation of Hawaiian–Emperor bend records major change in Pacific plate motion: *Science*, v. 313, p. 1281–1284, <https://doi.org/10.1126/science.128489>.

Sutherland, R., 1995, The Australia–Pacific boundary and Cenozoic plate motions in the SW Pacific: Some constraints from Geosat data: *Tectonics*, v. 14, p. 819–831, <https://doi.org/10.1029/95TC00930>.

Tarduno, J.A., et al., 2003, The Emperor Seamounts: Southward motion of the Hawaiian hotspot plume in earth's mantle: *Science*, v. 301, p. 1064–1069, <https://doi.org/10.1126/science.1086442>.

Wessel, P., and Kroenke, L.W., 2008, Pacific absolute plate motion since 145 Ma: An assessment of the fixed hot spot hypothesis: *Journal of Geophysical Research*, v. 113, B06101, <https://doi.org/10.1029/2007JB005499>.

Wessel, P., Harada, Y., and Kroenke, L.W., 2006, Towards a self-consistent, high-resolution absolute plate motion model for the Pacific: *Geochemistry Geophysics Geosystems*, v. 7, Q03L12, <https://doi.org/10.1029/2005GC001000>.

Printed in USA